Development, Growth & Differentiation

WILEY | JAPANESE SOCIETY OF DEVELOPMENTAL BIOLOGISTS

RESEARCH ARTICLE OPEN ACCESS

Transcriptome Comparison Between the Cultured and In Vivo Chick Primordial Germ Cells by SMART-Seq-Based Single-Cell RNA Sequencing

Yoshiki Hayashi[1] | Atsushi Doi[2] | Hiroko Iikawa[3] | Hirokazu Kimijima[4] | Yutaka Suzuki[5] | Akinori Kanai[5] | Hideki Hirakawa[6] | Daisuke Saito[1]

[1]Graduate School of Science, Kyushu University, Nishi-ku, Fukuoka, Japan | [2]Medical Institute of Bioregulation, Kyushu University, Higashi-ku, Fukuoka, Japan | [3]Graduate School of Systems Life Sciences, Kyushu University, Nishi-ku, Fukuoka, Japan | [4]Graduate School of Biostudies, Kyoto University, Sakyo-ku, Kyoto, Japan | [5]Life Science Data Research Center, Graduate School of Frontier Science, The University of Tokyo, Kashiwa, Chiba, Japan | [6]Graduate School of Bioresource and Bioenvironmental Science, Kyusyu University, Nishi-ku, Fukuoka, Japan

Correspondence: Yoshiki Hayashi (hayashi.yoshiki.904@m.kyushu-u.ac.jp) | Daisuke Saito (saito.daisuke.036@m.kyushu-u.ac.jp)

Received: 4 July 2025 | **Revised:** 23 December 2025 | **Accepted:** 22 January 2026

Keywords: chick | primordial germ cell | transcriptome

ABSTRACT

Primordial germ cells (PGCs), the precursors of the germline, have unique cellular characteristics to undergo long-distance migration to the embryonic gonads and have the potential to differentiate into somatic cells. Among the animal models studying PGC development, the chicken PGCs are an ideal model, since it is a rare model in which long-term PGC cultivation is applicable. Although the cultural applicability of chicken PGC makes it attractive for revealing the PGC character and its developmental processes, some differences from in vivo PGCs are known, such as the remarkable upregulation of cell proliferation and a lesser ability to reach the gonads. Understanding these differences at the molecular level is crucial. To this end, we first performed SMART-seq-based single-cell RNA sequencing to compare transcriptomes between in vivo PGCs and cultured PGCs. Our results revealed that PGC cultivation causes a shift from a MYC-dependent to a MYCN-dependent gene regulatory network (GRN) in PGCs, suggesting that this reprogramming contributes to the acquisition of proliferation ability and stem cell characteristics in cultured PGCs. Additionally, our results suggest that the MYCN-dependent GRN increases the risk of somatic differentiation, particularly in neural fate, in cultured PGCs. In addition, our transcriptome analysis identified a new cell population that shows molecular characteristics of germline-biased undifferentiated cells. Thus, our study provides fundamental molecular information to understand both the effects of PGC cultivation and the developmental process of chicken PGCs.

1 | Introduction

PGCs are the precursors of the germline and contribute to the life continuity of the species. In addition to their importance as the precursors of the cells in charge of transferring the inheritable materials to the next generation, PGCs have unique cellular and developmental characteristics rarely observed in other cell types in the somatic tissues. First, PGCs of some animal species, including insects and vertebrates, have been proven to have the potential to differentiate into somatic cells under some conditions (Hayashi et al. 2004; Gross-Thebing et al. 2017; Youngren et al. 2005). Thus, PGCs are potentiating to have stem cell-like characteristics. The second discriminating characteristic of PGCs is the ability to migrate long distances within the embryo (Richardson and Lehmann 2010). PGCs in most animal species studied are formed at early embryogenesis outside of the gonads, and migrate through several different circumstances to reach the embryonic gonads, where they eventually differentiate into gametes. During

[Correction added on 21 March 2026, after first online publication: The copyright line was changed.]'.

This is an open access article under the terms of the Creative Commons Attribution-NonCommercial License, which permits use, distribution and reproduction in any medium, provided the original work is properly cited and is not used for commercial purposes.

© 2026 The Author(s). *Development, Growth & Differentiation* published by John Wiley & Sons Australia, Ltd on behalf of Japanese Society of Developmental Biologists.

migration, PGCs need to maintain their germline fate with their fragile character as undifferentiated cells within the complicated developmental environment, and at the same time, they need to precisely accept migration cues from the outside to reach the gonads. Thus, PGCs are an ideal cellular model to investigate the mechanisms balancing the maintenance of cellular character and response to environmental signals. Avian PGCs, especially, provide a valuable model to address those matters for several reasons. First, Avian PGCs undergo migration via a unique route, the blood vessel (Nakamura et al. 2007; Saito et al. 2022; Ichikawa and Horiuchi 2023). Chicken PGCs, as an example, are localized in the central zone of the area pellucida, on the ventral surface of the epiblast (Embryonic day 0; E0). Those PGCs migrate anteriorly to the germinal crescent region where they enter the embryonic circulation associated with the formation of the blood vascular network at E1.25 (Murai et al. 2021). After circulation, PGCs arrested in the capillaries near the germinal epithelium undergo extravasation to be outside the vasculature at around E2.5 (Saito et al. 2022; Ando and Fujimoto 1983). PGCs then migrate along the dorsal mesentery to reach the embryonic gonads (E4.5). Thus, Avian PGCs undertake complicated cancer-like behavior to reach the gonads; they must proceed through intra- and extravasation for precise homing to the gonads.

The second merit of using chicken PGCs is the technical aspects; Chicken PGCs are the first and few PGCs that can be applied to long-term culture after primary isolation from the embryos (Whyte et al. 2015; Van De Lavoir et al. 2006). Those cultured PGCs (cPGCs) are easily propagated and are also able to produce the next generation when they are injected back into the embryos. In addition, those cPGCs are applicable to plasmid transfection, thus suitable for analyzing the gene functions involved in migration processes (Saito et al. 2022; Suzuki et al. 2023). Therefore, chicken PGCs provide an ideal model for understanding PGC characteristics and the molecular mechanisms regulating in vivo hematogenous migration processes in general.

Although the cPGCs are a useful tool, it has been known that the cPGCs have several different characteristics not observed in in vivo PGCs (endogenous PGCs: ePGCs). First, cPGCs have a stronger proliferation ability than ePGCs; cPGCs easily propagate to $\times 10^6$ order number within a few weeks from a few hundred of their sourced ePGCs (Whyte et al. 2015; Song et al. 2014; Nakamura et al. 2007). Second, cPGCs have less ability to be integrated into embryonic gonads than ePGCs; even when 10 times more cPGCs are injected back into the embryo, the contribution of the cPGCs to generate descendants is limited, suggesting that cPGCs are less competitive to reach the gonads than ePGCs (Song et al. 2014). This disability of cPGCs to make the next generation leads to innovative overcoming experimental techniques in which ePGCs are experimentally ablated from the host embryos, so that cPGCs have no competition with ePGCs for reaching the gonads (Trefil et al. 2017; Nakamura et al. 2010; Nakamura et al. 2012; Woodcock et al. 2019; Chen et al. 2023). Thus, even though cPGCs are a useful model, it is fundamentally important to understand the difference between cPGCs and ePGCs for future use of cPGCs in cellular and/or developmental PGC models.

To understand those characters, basic information about gene expression is essential. To date, several studies provide genome-wide gene expression information about chicken PGCs. For example, gene expression profiles of ePGCs are developmentally analyzed with bulk-RNA sequencing (RNA-seq) and single-cell RNA-seq (scRNA-seq) (Rengaraj, Cha, Lee, et al. 2022; Gong et al. 2024; Rengaraj, Cha, Park, et al. 2022; Ichikawa et al. 2022). Also, gene expression profiles of cPGCs are analyzed with RNA-seq and scRNA-seq (Gong et al. 2024; Zou et al. 2025). Although those studies provide important basic information to understand the differences between the ePGCs and cPGCs, there are several matters to consider when comparing the data. For example, those studies were performed independently with different PGC sources, genetic backgrounds, and sequencing platforms. In addition, about the scRNA-seq, all the above studies utilized droplet-based library construction (e.g., 10× Genomics Chromium system), which is known to have cost-effective performance but provides relatively less effective detection of gene expression. Thus, obtaining deep and fine gene expression profiles from comparative sources is important to understand the differences between ePGCs and cPGCs.

In this study, we performed Switching Mechanism at the 5′ end of RNA Transcript (SMART)-seq-based scRNA-seq to compare the gene expression profiles between ePGCs and cPGCs under the same laboratory conditions. Although less cost-effective and with a limited sample size, SMART-seq achieves high detectability of gene expression, especially for low-expressed genes, and can be applied to single-cell samples. Our SMART-seq-based scRNA-seq successfully showed high detectability for gene expression from each single PGC. Our gene regulatory network (GRN) analysis revealed that the MYC-dependent transcriptional network was the most affected target of PGC cultivation, and remodeling from MYC- to MYCN-dependent network is achieved during the establishment of cPGCs. Also, our results suggest that the MYCN-dependent GRN increases the risk of somatic differentiation, particularly in neural fate, in cPGCs. Finally, we provide molecular evidence suggesting that our previously developed methods of collecting PGCs based on Tomato-lectin (Iikawa et al. 2024) are useful tools for capturing cells with molecular signatures of germline-biased undifferentiated cells from the earliest embryonic stage. Thus, our study provides the fundamental molecular knowledge to understand the effects of PGC cultivation and to help us further understand PGC specification processes in avian species.

2 | Results and Discussion

2.1 | SMART-Seq-Based scRNA-Seq Achieves High Detectability of Gene Expression in Single PGC

To evaluate the effects of PGC cultivation, we collected 96 PGCs from embryos at E2.5, which is the source of PGC cultivation (ePGC_E2.5), and 48 cPGCs from each of the initiating periods of PGC cultivation (1 week after ePGCs are in culture medium; cPGC_1w) or period in which the cPGCs are well established (3 weeks after ePGCs are in culture medium; cPGC_3w), by using our previously developed methods for the efficient collection of PGCs: *Lycopersicon esculentum* (Tomato) lectin (LEL) based labeling of PGCs combined with Fluorescence-Activated Cell Sorting (FACS) (Iikawa et al. 2024). Our LEL-labeling methods have been shown to effectively collect PGCs from E2.5 embryos compared to the

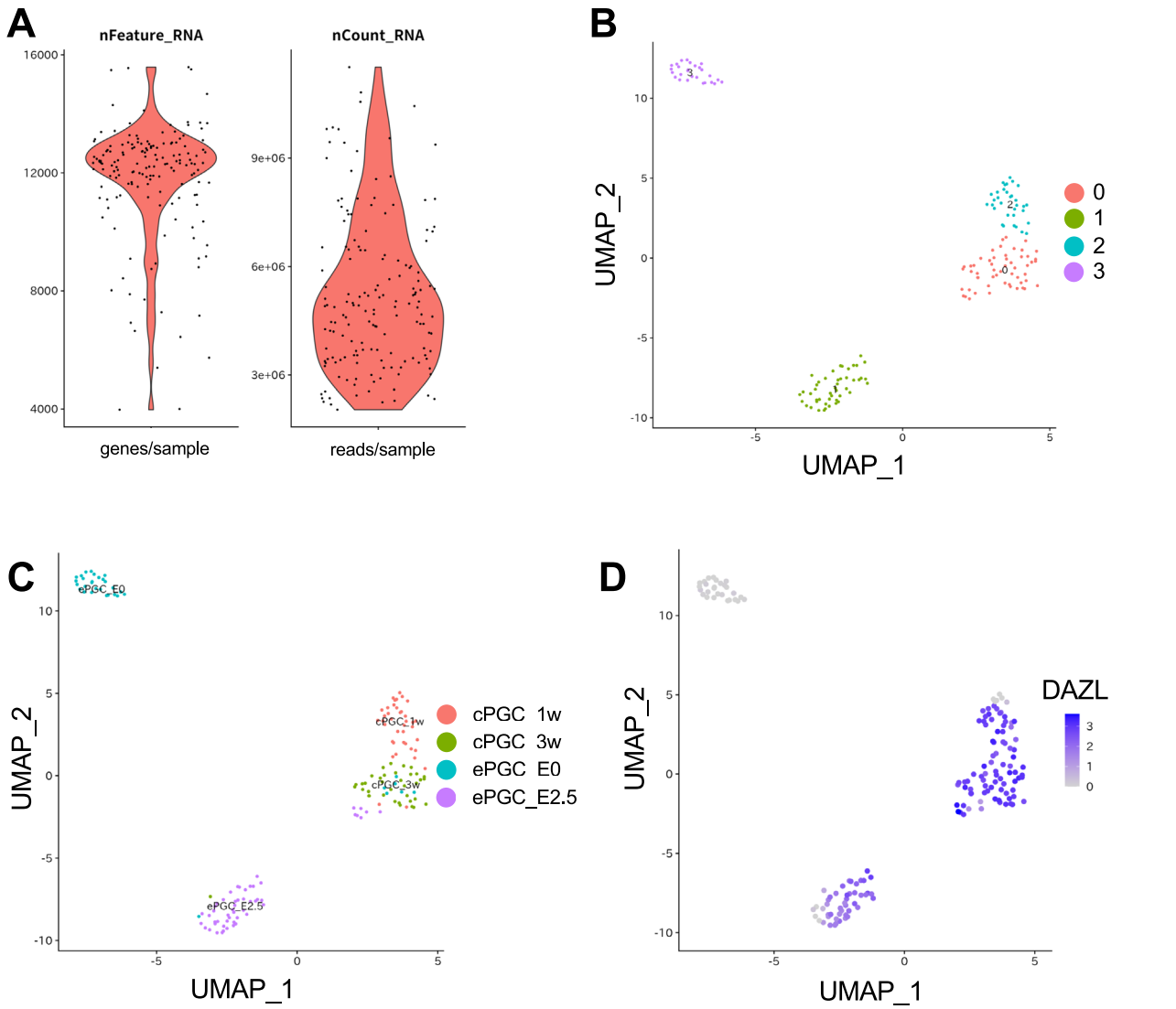

FIGURE 1 | Single-cell gene expression profiling of ePGCs and cPGCs. Gene expression profiles of in vivo PGCs and cultured PGCs were shown. (A) The Distribution of detected gene number (left) and number of obtained reads (right) from each cell is shown. (B, C) The Results of UMAP-based clustering analysis are shown. Our total samples were clustered into 4 clusters (B), with constituents of each cluster coming from the same sample category, except cluster 0 (C). (D) The Expression of DAZL, the germline marker, in each cell is shown. Color value is based on normalized log-transformed value.

method that depends on the PGC-labeling with SSEA1, which is a commonly used labeling method of PGCs (Jung et al. 2005). Previously, we showed that LEL-labeled PGCs consistently expressed the evolutionarily conserved PGC markers DEAD-box helicase 4 (DDX4) and Deleted in azoospermia-like (DAZL), but approximately half of LEL-labeled PGCs are not labeled with SSEA1, indicating that the LEL-labeling method is more efficient in collecting PGCs than the SSEA1 method. Also, our previous work showed that LEL methods label morphologically indistinguishable PGC-like cells from E0 stage embryos, which are absent from SSEA1. Although those results indicate the possibility that our LEL method could collect the PGCs from more prior embryonic stages than the SSEA1-methods, the lack of molecular information of those PGC-like cells prevents confirming the efficiency of the LEL method on this point. Thus, we determined to investigate the gene expression of those PGC-like cells additionally to evaluate the possibility that our LEL method could collect PGCs from the earliest embryonic stage. To this end, we additionally collected 99 LEL-positive PGC-like cells (ePGC_E0) and performed SMART-seq-based scRNA-seq. We sequenced all of the above libraries and evaluated the sample quality based on the number of genes detected. The number of genes detected from most of the samples was more than 12,000 genes (Figure 1A), which is obviously a higher number than 10× Genomics Chromium-based scRNA-seq, which detects a few thousand genes from chicken PGCs (such as in Zou et al. 2025), indicating the usefulness of our SMART-seq-based scRNA-seq. We set our sample cut-off to samples with 100 genes per sample, and as a result, we obtained a total of 162 samples for further analysis. Uniform manifold approximation and projection (UMAP) analysis showed our samples were clustered in four groups, with those roughly merged with their sample source, except ePGC_E0 (Figure 1B,C). Samples from ePGC_E0 were divided into two clusters (cluster 0 and 3 in Figure 1B), one of which was a cluster whose main constituent is ePGC_3w

samples (Cluster 0, Figure 1B,C). We confirmed the expression amplitude of DAZL among those samples and found that DAZL expression is the highest in cluster 0, and most of the samples in other clusters have moderate expression of DAZL, except cluster 3, which shows the lowest or absent expression of DAZL (Figure 1D). Those results showed that two populations of PGC-like cells from E0 embryos in different clusters have different characteristics for DAZL expression. In the following analysis, we referred to the names of each cluster as the main constituents of each cluster (Cluster 0 as cluster cPGC_3w_mix, Cluster 1 as ePGC_E2.5, Cluster 2 as cPGC_1w, Cluster 3 as ePGC_E0, Figure 1C).

2.2 | Marker Gene Comparison Revealed the Molecular Features of Each PGC Cluster

To investigate the gene expression character for each cluster, we identified marker genes of each cluster; genes whose expressions are significantly upregulated in one cluster compared to the others. Our clustering analysis of gene expression from each cluster successfully identified marker genes of each cluster (number of marker genes; cPGC_3w_mix: 2366 genes, ePGC_E2.5: 608 genes, cPGC_1w: 476 genes, ePGC_E0: 1412 genes. Top 10 marker genes are shown in Figure 2A, Table S1). To see the overall molecular trend of each cluster, we performed Gene Ontology (GO) enrichment analysis and KEGG pathway analysis using marker genes (Figure 2B–E, Figure S1A–F). Our GO enrichment analysis showed that ePGC_E2.5, which is the source of cPGCs, has upregulation of genes with GO (BP: Biological Processes) related to heme and its constituents (Figure 2B) (porphyrin, belonging to the tetrapyrrole group, is a constituent of heme). Also, marker genes of ePGC_E2.5 showed enrichment of GO (BP) related to oxygen metabolism (reactive oxygen species metabolic process and oxygen transport). ePGC_E2.5 marker genes also have mitochondria-related GOs in the GO categories (MF: Molecular Functions, CC: Cellular Components) (Figure S1A,B, KEGG pathway analysis is in Figure S1C). These enriched GOs were related to mitochondrial activity, suggesting that PGCs of embryonic day 2.5 have higher mitochondrial activity than other conditions. Since we isolated the ePGC_E2.5 from the blood vessel of a chicken embryo, we also checked whether the detection of heme-related GOs in this cluster is due to contamination by blood cells. To this end, we checked the expression of genes contributing to both heme and tetrapyrrole metabolism GO categories; these categories include 6 of the 10 GO categories detected in the ePGC_E2.5 cluster (Figure S3A–D). The expression of the analyzed genes was broadly detected in cells constituting the cPGC_E2.5 cluster (Figure S3A–D) and was well aligned with germline gene expression, Dazl and DDX4 (Figures 1D and 4A). Thus, it is less possible that the detection of those GOs was caused by contamination of blood cells.

GO enrichment analysis for cPGC_1w was less informative, but KEGG pathway analysis for those marker genes showed that mitophagy and ferroptosis pathways were upregulated in this cell population (Figure 2C), suggesting that removal of mitochondrial and causal release of iron ions occur during the first step of PGC cultivation. It is possible that metabolic reprogramming from mitochondrial oxidative phosphorylation (OXPHOS) to glycolysis, which is frequently observed in proliferating cells (Deberardinis et al. 2008), occurs in the initiation step of PGC cultivation. GO enrichment analysis for cPGC_3w_mix marker genes showed most of the GO (BP)s enriched in this population were related to cell morphology, especially to the formation of cellular projections, such as neuron projection (Figure 2D). To evaluate whether a particular cell population causes differentiation to neural cells, we examined the expression of genes related to the neural development GO category (axon guidance [SLIT1, GAP43], synapse formation [LRRC3C], and transcriptional factor [TF] regulating motor neuron development [MNR2]) (Figure S3E–H). Although all observed genes are upregulated in the cPGC_3w_mix population with heterogeneous intensities, no cell population expresses all of those genes simultaneously. Given that those cells express certain levels of germline genes, DAZL and DDX4 (Figures 1D and 4A), cPGC_3w_mix cells maintain PGC character with slight enhancement of differentiation. Those results also suggest that established PGCs partially possess the molecular characteristics of other cell lineages, such as the neuronal cell lineage. Finally, we performed GO enrichment analysis for the ePGC_E0 cluster (Figure 2E), which is absent for DAZL expression (Figure 1D). GO enrichment analysis for this cell population revealed that GO (BP)s related to translation (e.g., ribosome biogenesis) and post-transcriptional regulation (e.g., ribonucleoprotein complex biogenesis) were enriched in marker genes of the ePGC_E0 cluster. GO enrichment analysis of other GO categories (MF and CC) and KEGG pathway analysis also suggest the enhancement of translational regulation in this cell population (Figure S1D–F). Since the regulation of maternally inherited RNA is critical in cells in early embryonic stages, these results might reflect the cellular status of those developmental situations.

2.3 | Cultivation Affects the MYC-Dependent Gene Regulatory Network in PGCs

Next, we determined to compare the gene expression profile of ePGCs and cPGCs in depth to evaluate the effects of PGC cultivation. To this end, we directly compared the gene expression profiles between ePGC_E2.5 and cPGC_1w based on sample origin rather than clusters. We detected 1148 differentially expressed genes (DEGs) in cPGC_1w (747 upregulated and 401 downregulated) compared to ePGC_2.5 (Figure 3A). We found that one of the top downregulated genes in cPGC_1w was MYC (Figure 3A, approximately 40-fold downregulation, Table S2, Figure S2C), which is the well-known TF involved in regulation of cell pluripotency and cell proliferation (Whitfield and Soucek 2025; Bretones et al. 2015; Chappell and Dalton 2013; Kim et al. 2010). The GRN analysis between TFs and target genes for those DEGs showed that MYC is a top hub TF in that GRN (Figure 3C, Table S3), emphasizing the importance of downregulation of MYC-dependent GRN in the initial period of PGC cultivation. About the target genes, we observed upregulation of CDKN1A/p21, which is a cyclin-dependent kinase inhibitor to repress the cell cycle (Karimian et al. 2016), and is known to be a repressive target of MYC (Bretones et al. 2015; Wu et al. 2003). Those observations suggest that MYC-dependent GRN works in PGCs. Interestingly, GATA6, which is the endoderm master regulator and key

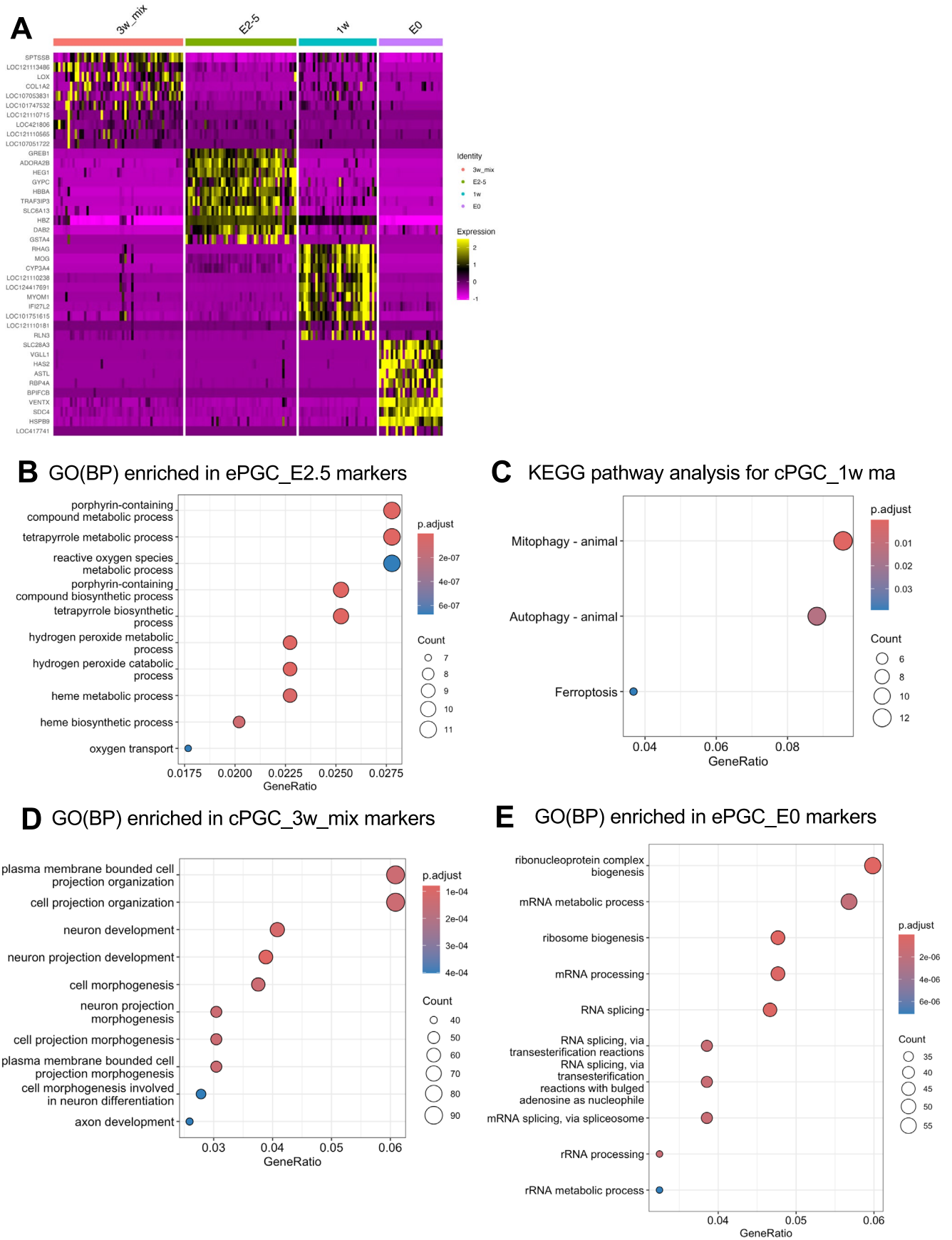

FIGURE 2 | Legend on next page.

FIGURE 2 | Molecular feature of PGC clusters. (A) The heat map of the top 10 marker genes for each cluster is shown. The labels on the top show the original clusters, and the labels on the left indicate the names of marker genes. (B–E) The results of Gene Ontology (GO) enrichment analysis or KEGG pathway analysis for marker genes of each cluster are shown. The analyzed marker gene source and type of analysis are indicated at the top of each figure (e.g., GO(BP) enriched in ePGC_E2.5 markers means the results of GO enrichment analysis for Biological Process (BP) for marker genes of the ePGC_E2.5 cluster).

repressive target of MYC in pluripotent stem cells, was upregulated in this condition (Figure 3C) (Smith et al. 2010), suggesting that PGCs in the initial cultivation period lose their stem cell-like character. We also noticed a small population of cPGC_1w cells show low expression of germline genes (DAZL, DDX4, PIWIL1, DND1, Figures 1D and 4A–D, respectively) and pluripotent genes (OCT4, NANOG, Figure 4F,G) simultaneously, suggesting that part of PGCs lose their germline and stem cell-like character, and fail to be established as cPGCs. Thus, our transcriptome comparison strongly suggests that the loss of stem cell-like character of ePGCs occurs in the initial step of PGC cultivation. MYC is well known as a repressive target of Smad3 (Chen et al. 2002); the downstream signal transducer of Activin A, which is one of the three constituent ligands of PGC cultivation medium (Whyte et al. 2015). Although the signaling pathways regulated by both of other two of three constituent ligands, Insulin contained in B27 supplement and FGF2 are known to be involved in upregulation of MYC (Sears et al. 2000; Lee et al. 2022), our results suggest that Activin A-dependent TGF-beta signaling has strong effects on the PGC state alternation occurring in the initial step of PGC cultivation. Next, we compared the gene expression profiles between ePGC_E2.5 and cPGC_3w, and between cPGC_1w and cPGC_3w. We detected a total of 2459 genes that were differentially expressed in cPGC_3w (1963 upregulated genes and 496 downregulated genes) compared to ePGC_2.5 (Figure 3B, Table S4), and a total of 635 genes (292 upregulated and 343 downregulated) compared to cPGC_1w (Figure S2A, Table S6). As in the case of cPGC_1w, MYC was significantly downregulated in cPGC_3w (approximately 24-fold upregulation, Table S4, Figure S2C). Our GRN analysis on DEGs based on TFs and their known targets revealed that MYC was the first top hub TFs in the GRN of DEGs (Figure 3D, Table S5), suggesting that MYC-dependent GRN still affected by cultivation. Interestingly, we found that expression of MYCN, a MYC family gene which has functional and structural similarity to MYC (Chappell and Dalton 2013), is upregulated in cPGC_3w (Figure 3D, Table S4, Figure S2D). Upregulation of MYCN in PGCs occurs during the cultivation, since transcriptome comparison between cPGC_1w and cPGC_3w detects MYCN as a differentially expressed gene (Figure S2A, Table S6). The GRN analysis on DEGs between cPGC_1w and cPGC_3w showed that MYCN-dependent network formed (Figure S2B). We found downregulation of CDKN1A/p21 occurs during the cultivation period between 1 week and 3 weeks (Figure S2B), suggesting that re-acquisition of proliferation ability could occur during this period, probably in a MYCN-dependent manner (Figure S2B). MYCN is known to be involved in the regulation of cellular pluripotency, similar to MYC (Chappell and Dalton 2013). Interestingly, we observed upregulation of OCT4/Pou5f3 and NANOG occur in cPGC_3w (Figure 3D, Tables S4 and S6). Conversely, we found GATA6 is downregulated in cPGC_3w (Figure 2B, Table S6). Those observations strongly suggest that PGCs cultured for 3 weeks re-acquire the proliferation ability and pluripotent character in a MYCN-dependent manner. It has been shown that the forced expression of MYCN in chicken neural crest cells induces CNS-like neural stem cell characteristics in these cells (Kerosuo et al. 2018). Indeed, enrichment analysis of DEGs between the cPGC_1w and cPGC_3w using the ARCHS4_Tissues database revealed that DEGs were significantly enriched for those highly expressed in neural cells (Table S7), suggesting that cPGCs partially possess the neural cell character in gene expression level. This observation is consistent with the GO enrichment analysis for marker genes of cluster cPGC_3w_mix shown above. Therefore, our results suggest that shifting to MYCN-dependent GRN in cPGCs contributes to the maintenance of cell proliferation and stem cell character, but at the same time, it induces neural cell-like character in those. This phenomenon could account for why the cPGCs show less competitiveness to reach the embryonic gonads compared to ePGCs.

2.4 | E0 PGC-Like Cells Express Genes Regulating Pluripotency and Germline Development

Finally, we investigated the molecular characteristics of PGC-like cells identified from our LEL-based labeling. Our previous work showed that LEL-labeled PGC-like cells from embryonic day 0 have morphology identical to PGC but are absent from SSEA1 (Iikawa et al. 2024). FACS analysis in this study showed that the LEL-labeled PGC-like cells constitute approximately 30% of E0 epiblast cells (29.9%, 125 lectin-positive cells/418 analyzed epiblast cells). Our clustering analysis showed that those PGC-like cells are separately integrated into two clusters; one is absent for DAZL (cluster ePGC_E0), and one is merged into cluster cPGC_3w_mix (Figure 1C,D). These results indicate that the LEL-labeled cell population contains cells with PGC morphology but without DAZL expression (ePGC_E0 cluster). To evaluate whether these PGC-like cells in ePGC_E0 cluster possess the molecular signature of germline and/or undifferentiated cells, we checked the expression of genes related to cellular pluripotency (OCT4/Pou5f3, NANOG, SOX2, KLF4, LIN28A, LIN28B, Figure 4F–I, Figure S4E,F) and germline development (DDX4/VASA, NANOS1, NANOS3, PIWIL1, DAZL, DND1, PRDM14, KIT, TDRD9, PRDM1, Figures 1D and 4A–E, Figure S4A–D). We found that the cells in cluster ePGC_E0 showed low level but certain expression of several germline genes (DDX4: Figure 4A, PRDM14: Figure 4E, KIT: Figure S4A, TDRD9: Figure S4B, NANOS1: Figure S4C, PRDM1: Figure S4D) with high expression of pluripotent marker genes (such as OCT4/Pou5f3 and NANOG in Figure 4F,G). Of note, we observed that PRDM1, which functions as a prerequisite for PGC specification in mammals, showed higher expression than other

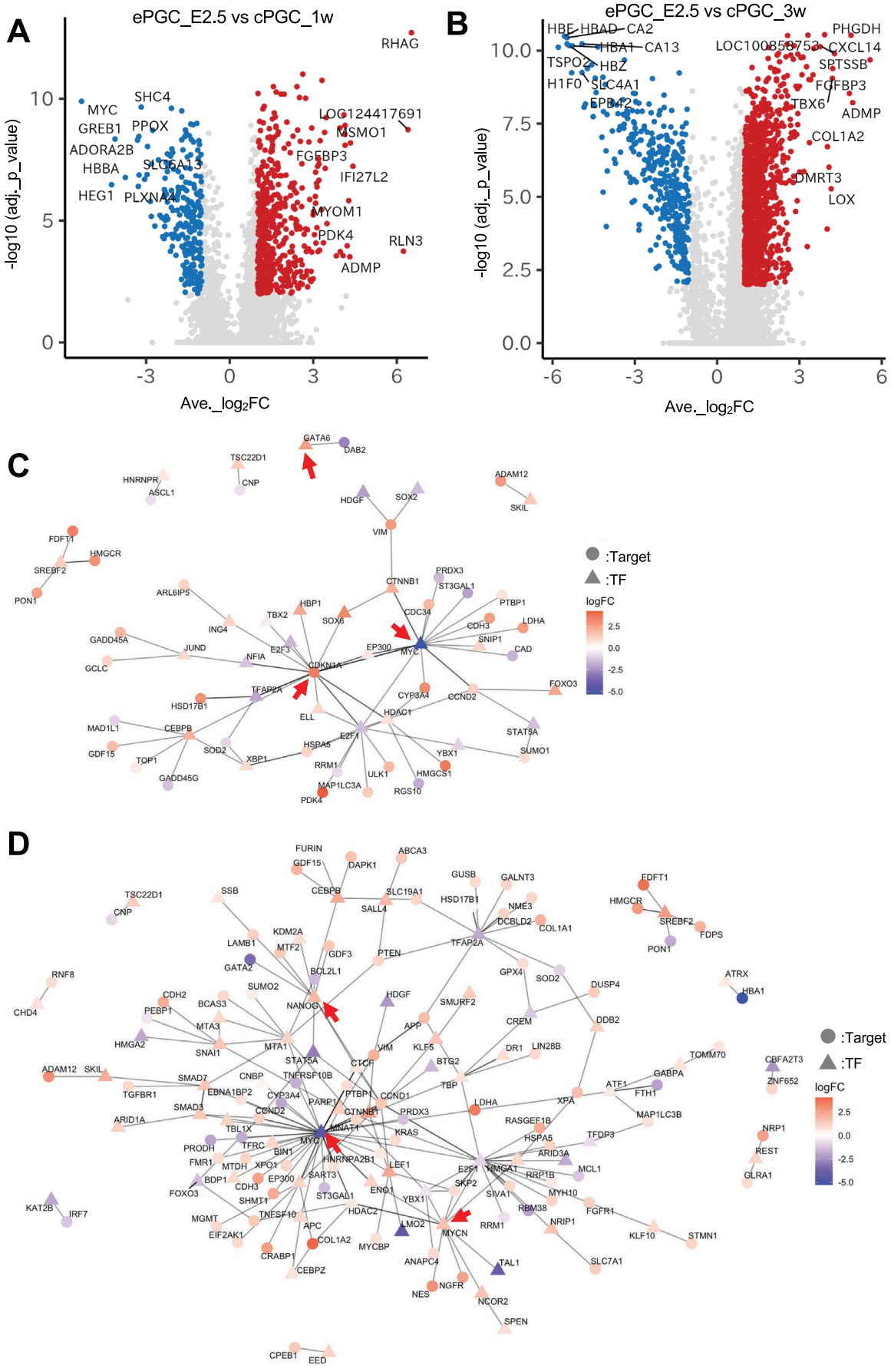

FIGURE 3 | Legend on next page.

FIGURE 3 | Gene expression comparison between ePGCs and cPGCs. (A, B) Volcano plots of differentially expressed genes (DEGs) by comparison between ePGC_E2.5 and cPGC_1w (A), or ePGC_E2.5 and cPGC_3w (B) are shown. In both of those analyses, ePGC_E2.5 samples are set as controls. Red plots indicate the upregulated genes (average log2FC > 1, adjusted *p*-value < 0.01) and blue plots indicate the downregulated genes (average log2FC < −1, adjusted *p*-value < 0.01). (C, D) Gene regulatory network (GRN) analysis for DEGs based on the relation between transcriptional factors (TFs, indicated as triangles) and their known target genes (Target, indicated as circles) is shown. (C) GRN analysis for DEGs from comparison of ePGC_E2.5 and cPGC_1w. (D) GRN analysis for DEGs from comparison of ePGC_E2.5 and cPGC_3w. In both (C) and (D), the color value of the nodes indicates the $\log_2$FC of DEGs. Red arrows in (C) and (D) indicate the genes discussed in main texts.

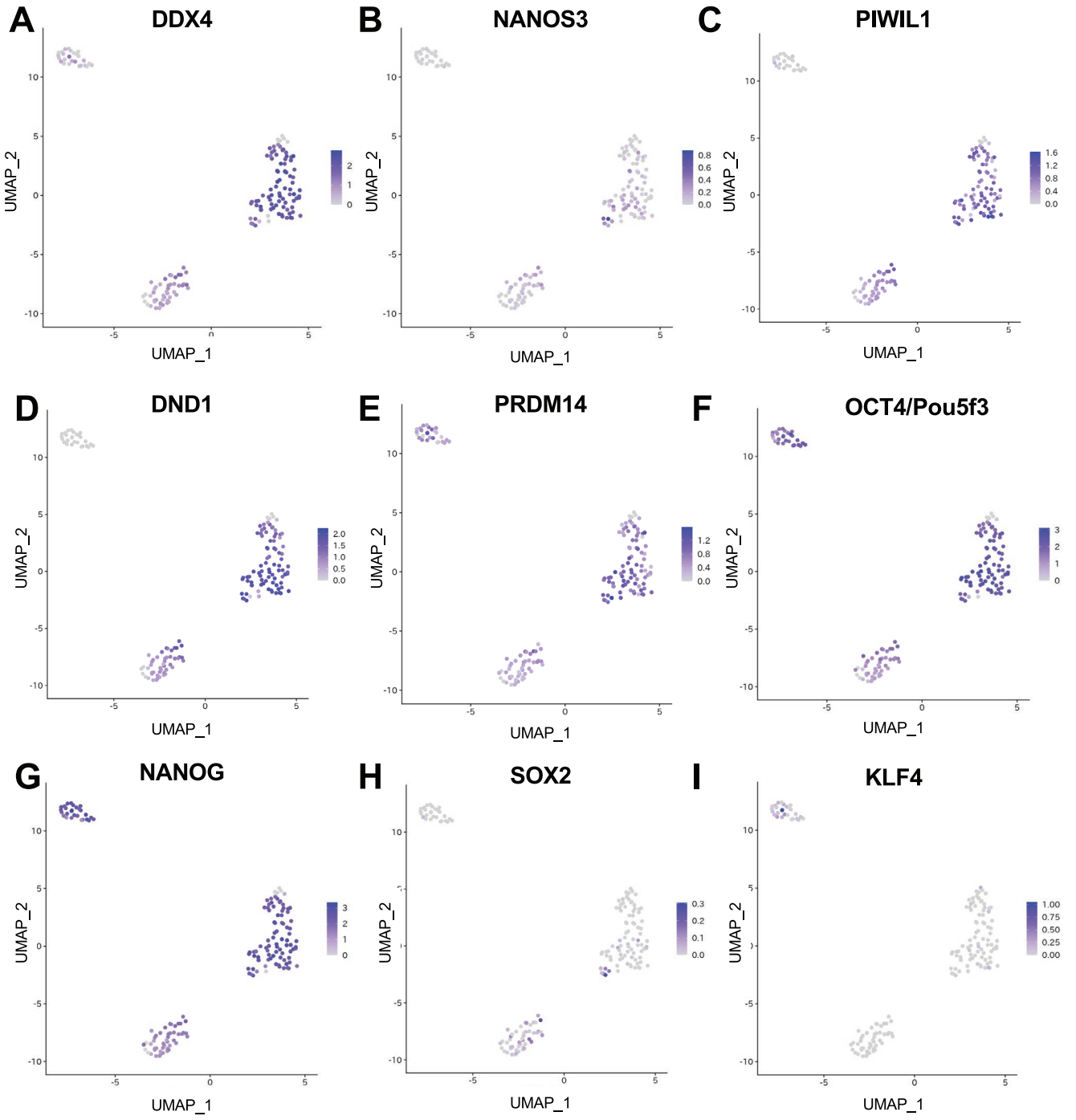

FIGURE 4 | Molecular characterization of PGC-like cells. The expression level of indicated germline genes (A–E) and pluripotent marker genes (F–I) in each sample is shown. Color value is based on normalized log-transformed value.

germline genes (Figure S4D). These data suggest that the PGC-like cell population cluster includes cells with characteristics of germline-biased undifferentiated cells. A previous study showed that ectopic expression of DDX4 in chick early epiblast cells can drive the germline fate in those cells (Lavial et al. 2009), indicating that germline-competent cells are present in chick early epiblasts. In addition, a recent study by Chen et al. (2025) showed that chicken PGCs can be derived from chicken embryonic stem cells without forced expression of maternal factors. Taken together, our observations suggest that the PGC-like cells found in the E0 embryos, which highly express pluripotent genes and PRDM1, are the germline-biased undifferentiated cells. Compared with other animal models, the understanding of PGC specification in avian species is less well developed, as there are no methods to collect PGCs from early embryos. Previous works depend on SSEA1-labeling or fluorescent-tagged DAZL expression for collecting PGCs (Ichikawa and Horiuchi 2023; Rengaraj, Cha, Lee, et al. 2022; Rengaraj, Cha, Park, et al. 2022), but both of those markers are absent in our LEL-positive PGC-like cells (Iikawa et al. 2024). DDX4/VASA is shown to be the earliest marker for PGC, but a fluorescent-tagged DDX4 transgenic strain is not yet available (Tsunekawa et al. 2000). Thus, our results showed that our developed LEL-labeling methods provide a chance to collect PGC-like cell populations those on the PGC specification processes and provide a first chance to understand the molecular mechanism regulating PGC specification in avian species.

The PGC cultivation system in chickens is valuable for revealing the molecular mechanism regulating unique PGC characters, such as their stem cell-like potential and long-distance migration. In this study, we first provide the molecular evidence to understand the effects of PGC cultivation with SMART-seq-based deep sequencing at the single-cell level. Our study suggests that shifting to MYCN-dependent GRN is essential for the success of PGC cultivation. Also, our study provides the risk of somatic differentiation by cultivation conditions. These results suggest that establishing conditions that simultaneously support reprogramming into a MYCN-dependent GRN promoting both cell proliferation and maintenance of stem cell identity, while inhibiting somatic differentiation, is essential for successful PGC cultivation. To date, PGC cultivation has not been successful in many animals, including avian species. Thus, our study provides the strategic direction and molecular targets to achieve PGC cultivation in other avian species. During the preparation of this manuscript, Doddamani and colleagues reported the long-term cultivation method of goose PGCs (Doddamani et al. 2025). The study revealed that Activin A and FGF2 have opposite effects on goose PGC in vitro propagation; excessive Activin A inhibits propagation of PGCs (Doddamani et al. 2025). This observation is consistent with our results suggesting that Activin A signaling through SMAD3 function suppresses MYC-dependent GRN, and emphasizes the importance of balancing the activity of three major constituents, Activin A, FGF2, and Insulin. In addition to the molecular differences between ePGCs and cPGCs, our study provides molecular evidence suggesting that our LEL-labeling method is a useful tool for collecting PGCs from the early stage of the chicken embryo. Although the specification process of PGC is a fundamental question of developmental biology and is known to be diverse among animal species, PGC specification processes in avian species are less understood because of the lack of molecular information. Our study suggests that the LEL-positive PGC-like cells at embryonic day 0 are a partially differentiated cell population in the germline. Thus, our results and developed methods could be a key to understanding the PGC specification processes in avian species. Therefore, our SMART-seq-based scRNA-seq analysis provides fundamental knowledge not only for the future success of PGC cultivation in non-chicken animals but also for understanding the PGC specification processes in avian species.

3 | Materials and Methods

3.1 | Animals

Fertilized eggs from the BL-E strain of brawn leghorn chicken were provided by Nagoya University through the National Bio-Resource Project of the MEXT, Japan. The eggs were incubated at 38.5°C in a high-humidity chamber (50%–60%). Chicken embryos at stages E0 and E2.5 were dissected and collected after 30 min and 60 h of incubation, respectively. All animal experiments were conducted in accordance with the ethical guidelines for animal experimentation established by Kyushu University.

3.2 | PGC Culture

PGCs collected from E2.5 chicken embryos were cultured as described previously (Iikawa et al. 2024). In brief, the PGCs were cultured in modified FACS medium at 38.0°C with 5% CO_2 in humidity incubator until the investigated time points (1 week or 3 weeks). The FACS medium composition includes; 65.5% DMEM (high glucose, Ca^{2+}-free, no-glutamine) (Nakarai tesque, Japan), 21.8% Deionized Distilled Water (DDW) (Fuji film, Japan), 1× Nucleotides (Merck-Millipore, USA), 2.0 mM GlutaMax (Thermo Fisher Scientitic [Thermo], USA), 1.2 mM Sodium Pyruvate (Thermo), 1× NEAA (Thermo), 55 μM beta-mercaptoethanol (Fujifilm), 1% Penicillin–Streptomycin-Amphotericin (PSA) (Fuji film), 2% B27 Supplements (Thermo), 0.2% Chicken Serum (Biowest, France), 0.1 mg/mL Heparin (Sigma-Aldrich, USA), 2 mg/mL Ovoalbmin (Sigma-Aldrich), 25 ng/mL Activin A (API, Japan), 4 ng/mL FGF Chimera (Fuji film), 100 μM $CaCl_2$ (Nakalai tesque) (Whyte et al. 2015). Half of the medium was replaced with fresh medium every 2 days.

3.3 | PGC Collection

PGCs from E0 and E2.5 embryos were collected by labeling with LEL conjugated with DyLight488 (DL-1174, Vector Laboratories, USA) by FACS (SH800, Sony, Japan) as previously described (Iikawa et al. 2024). Sorted cells were collected in a 96-well plate (Ro-bind, 0030 129.504, Eppendorf, Germany) filled with Lysis Buffer containing RNase inhibitor (Components of kit described below, TAKARA, Japan) and immediately frozen with dry ice. The lysed cells were used to prepare the libraries as described below.

3.4 | SMART-Seq

The SMART-seq libraries were prepared with SMART-seq Single-Cell PLUS Kit (TAKARA) following the manufacturer's instruction. The libraries were sequenced by NovaSeq 6000 with 150 bp pair-end sequencing (Illumina).

3.5 | Data Analysis

The treated reads were mapped with chicken genome (bGalGal1.mat.broiler.GRCg7b). The cluster analysis was performed with Seurat software (5.1.0) on R (4.4.1). GO term enrichment analysis was performed with clusterProfiler (4.15.1) on R (4.5.0), and enrichment analysis to identify tissue-specific gene expression signatures in the DEGs was performed with enrichR (3.4) with ARCHS4_Tissues gene sets on R (4.5.0). Network analysis was performed with igraph (2.1.4) on R (4.5.0). The network data were obtained from TRRUST version2 (human), and chick differentially expressed genes were converted to human ortholog by using g:Profiler web tool.

Author Contributions

D.S. designed the experiments. H.I., Y.S. and A.K. performed the experiments. Y.H., A.D. and H.H. analyzed the data. Y.H. and D.S. wrote the manuscript. All authors discussed the results and commented on the manuscript.

Acknowledgments

This work was supported in part by Grants-in-Aid for Scientific Research from Japan Society for the Promotion of Science (JSPS) (KAKENHI Grant Number: 23K05777, 23K17933 to Y.H., and 22H02634, JP22H04925[PAGS]) to D.S. While preparing this work, the authors utilized the Grammarly web tool to verify the accuracy of English grammar. After using this tool, the authors reviewed and edited the content as needed and took full responsibility for the content of the published article.

Funding

This work was supported by the Japan Society for the Promotion of Science (23K05777, 23K17933, 22H02634, JP22H04925[PAGS]).

Conflicts of Interest

The authors declare no conflicts of interest.

Data Availability Statement

The data that support the findings of this study are openly available in DDBJ at https://www.ddbj.nig.ac.jp/index-e.html, reference number PRJDB17925.

References

Ando, Y., and T. Fujimoto. 1983. "Ultrastructural Evidence That Chick Primordial Germ Cells Leave the Blood-Vascular System Prior to Migrating to the Gonadal Anlagen: (Germ Cells/Chick/Migration/Ultrastructure)." *Development, Growth & Differentiation* 25: 345–352.

Bretones, G., M. D. Delgado, and J. Leon. 2015. "Myc and Cell Cycle Control." *Biochimica et Biophysica Acta* 1849: 506–516.

Chappell, J., and S. Dalton. 2013. "Roles for MYC in the Establishment and Maintenance of Pluripotency." *Cold Spring Harbor Perspectives in Medicine* 3: a014381.

Chen, C. R., Y. Kang, P. M. Siegel, and J. Massagué. 2002. "E2F4/5 and p107 as Smad Cofactors Linking the TGFbeta Receptor to c-Myc Repression." *Cell* 110: 19–32.

Chen, X., Z. Guo, X. Tong, et al. 2025. "Derivation of Embryonic Stem Cells Across Avian Species." *Nature Biotechnology*. https://doi.org/10.1038/s41587-025-02833-3.

Chen, Y. C., D. Saito, T. Suzuki, and T. Takemoto. 2023. "An Inducible Germ Cell Ablation Chicken Model for High-Grade Germline Chimeras." *Development* 150: dev202079.

Deberardinis, R. J., J. J. Lum, G. Hatzivassiliou, and C. B. Thompson. 2008. "The Biology of Cancer: Metabolic Reprogramming Fuels Cell Growth and Proliferation." *Cell Metabolism* 7: 11–20.

Doddamani, D., B. Lazar, K. Ichikawa, et al. 2025. "Propagation of Goose Primordial Germ Cells In Vitro Relies on FGF and BMP Signalling Pathways." *Communications Biology* 8: 301.

Gong, W., Y. Zou, X. Liu, et al. 2024. "Comparison of Primordial Germ Cell Differences at Different Developmental Time Points in Chickens." *Animal Bioscience* 37: 1873–1886.

Gross-Thebing, T., S. Yigit, J. Pfeiffer, et al. 2017. "The Vertebrate Protein Dead End Maintains Primordial Germ Cell Fate by Inhibiting Somatic Differentiation." *Developmental Cell* 43: 704–715.e705.

Hayashi, Y., M. Hayashi, and S. Kobayashi. 2004. "Nanos Suppresses Somatic Cell Fate in Drosophila Germ Line." *Proceedings of the National Academy of Sciences of the United States of America* 101: 10338–10342.

Ichikawa, K., and H. Horiuchi. 2023. "Fate Decisions of Chicken Primordial Germ Cells (PGCs): Development, Integrity, Sex Determination, and Self-Renewal Mechanisms." *Genes (Basel)* 14: 612. https://doi.org/10.3390/genes14030612.

Ichikawa, K., Y. Nakamura, H. Bono, R. Ezaki, M. Matsuzaki, and H. Horiuchi. 2022. "Prediction of Sex-Determination Mechanisms in Avian Primordial Germ Cells Using RNA-Seq Analysis." *Scientific Reports* 12: 13528.

Iikawa, H., A. Nishina, M. Morita, Y. Atsuta, Y. Hayashi, and D. Saito. 2024. "Labeling and Sorting of Avian Primordial Germ Cells Utilizing *Lycopersicon esculentum* Lectin." *Development, Growth & Differentiation* 66: 452–461.

Jung, J. G., D. K. Kim, T. S. Park, S. D. Lee, J. M. Lim, and J. Y. Han. 2005. "Development of Novel Markers for the Characterization of Chicken Primordial Germ Cells." *Stem Cells* 23: 689–698.

Karimian, A., Y. Ahmadi, and B. Yousefi. 2016. "Multiple Functions of p21 in Cell Cycle, Apoptosis and Transcriptional Regulation After DNA Damage." *DNA Repair (Amst)* 42: 63–71.

Kerosuo, L., P. Neppala, J. Hsin, et al. 2018. "Enhanced Expression of MycN/CIP2A Drives Neural Crest Toward a Neural Stem Cell-Like Fate: Implications for Priming of Neuroblastoma." *Proceedings of the National Academy of Sciences of the United States of America* 115: E7351–E7360.

Kim, J., A. J. Woo, J. Chu, et al. 2010. "A Myc Network Accounts for Similarities Between Embryonic Stem and Cancer Cell Transcription Programs." *Cell* 143: 313–324.

Lavial, F., H. Acloque, E. Bachelard, M. A. Nieto, J. Samarut, and B. Pain. 2009. "Ectopic Expression of Cvh (Chicken Vasa Homologue) Mediates the Reprogramming of Chicken Embryonic Stem Cells to a Germ Cell Fate." *Developmental Biology* 330: 73–82.

Lee, J. S., M. W. Lero, J. Mercado-Matos, et al. 2022. "The Insulin and IGF Signaling Pathway Sustains Breast Cancer Stem Cells by IRS2/PI3K-Mediated Regulation of MYC." *Cell Reports* 41: 111759.

Murai, H., M. Shibuya, R. Kishita, C. Sunase, K. Tamura, and D. Saito. 2021. "Envelopment by Endothelial Cells Initiates Translocation of Avian Primordial Germ Cell Into Vascular Tissue." *Developmental Dynamics* 250: 1410–1419.

Nakamura, Y., F. Usui, D. Miyahara, et al. 2012. "X-Irradiation Removes Endogenous Primordial Germ Cells (PGCs) and Increases Germline Transmission of Donor PGCs in Chimeric Chickens." *Journal of Reproduction and Development* 58: 432–437.

Nakamura, Y., F. Usui, T. Ono, et al. 2010. "Germline Replacement by Transfer of Primordial Germ Cells Into Partially Sterilized Embryos in the Chicken." *Biology of Reproduction* 83: 130–137.

Nakamura, Y., Y. Yamamoto, F. Usui, et al. 2007. "Migration and Proliferation of Primordial Germ Cells in the Early Chicken Embryo." *Poultry Science* 86: 2182–2193.

Rengaraj, D., D. G. Cha, H. J. Lee, et al. 2022. "Dissecting Chicken Germ Cell Dynamics by Combining a Germ Cell Tracing Transgenic Chicken Model With Single-Cell RNA Sequencing." *Computational and Structural Biotechnology Journal* 20: 1654–1669.

Rengaraj, D., D. G. Cha, K. J. Park, K. Y. Lee, S. J. Woo, and J. Y. Han. 2022. "Finer Resolution Analysis of Transcriptional Programming During the Active Migration of Chicken Primordial Germ Cells." *Computational and Structural Biotechnology Journal* 20: 5911–5924.

Richardson, B. E., and R. Lehmann. 2010. "Mechanisms Guiding Primordial Germ Cell Migration: Strategies From Different Organisms." *Nature Reviews. Molecular Cell Biology* 11: 37–49.

Saito, D., R. Tadokoro, A. Nagasaka, et al. 2022. "Stiffness of Primordial Germ Cells Is Required for Their Extravasation in Avian Embryos." *iScience* 25: 105629.

Sears, R., F. Nuckolls, E. Haura, Y. Taya, K. Tamai, and J. R. Nevins. 2000. "Multiple Ras-Dependent Phosphorylation Pathways Regulate Myc Protein Stability." *Genes & Development* 14: 2501–2514.

Smith, K. N., A. M. Singh, and S. Dalton. 2010. "Myc Represses Primitive Endoderm Differentiation in Pluripotent Stem Cells." *Cell Stem Cell* 7: 343–354.

Song, Y., S. Duraisamy, J. Ali, et al. 2014. "Characteristics of Long-Term Cultures of Avian Primordial Germ Cells and Gonocytes." *Biology of Reproduction* 90: 15.

Suzuki, K., S. J. Kwon, D. Saito, and Y. Atsuta. 2023. "LIN28 Is Essential for the Maintenance of Chicken Primordial Germ Cells." *Cells and Development* 176: 203874.

Trefil, P., D. Aumann, A. Koslova, et al. 2017. "Male Fertility Restored by Transplanting Primordial Germ Cells Into Testes: A New Way Towards Efficient Transgenesis in Chicken." *Scientific Reports* 7: 14246.

Tsunekawa, N., M. Naito, Y. Sakai, T. Nishida, and T. Noce. 2000. "Isolation of Chicken Vasa Homolog Gene and Tracing the Origin of Primordial Germ Cells." *Development* 127: 2741–2750.

Van De Lavoir, M. C., J. H. Diamond, P. A. Leighton, et al. 2006. "Germline Transmission of Genetically Modified Primordial Germ Cells." *Nature* 441: 766–769.

Whitfield, J. R., and L. Soucek. 2025. "MYC in Cancer: From Undruggable Target to Clinical Trials." *Nature Reviews. Drug Discovery* 24: 445–457.

Whyte, J., J. D. Glover, M. Woodcock, et al. 2015. "FGF, Insulin, and SMAD Signaling Cooperate for Avian Primordial Germ Cell Self-Renewal." *Stem Cell Reports* 5: 1171–1182.

Woodcock, M. E., A. A. Gheyas, A. S. Mason, et al. 2019. "Reviving Rare Chicken Breeds Using Genetically Engineered Sterility in Surrogate Host Birds." *Proceedings of the National Academy of Sciences of the United States of America* 116: 20930–20937.

Wu, S., C. Cetinkaya, M. J. Munoz-Alonso, et al. 2003. "Myc Represses Differentiation-Induced p21CIP1 Expression via Miz-1-Dependent Interaction With the p21 Core Promoter." *Oncogene* 22: 351–360.

Youngren, K. K., D. Coveney, X. Peng, et al. 2005. "The Ter Mutation in the Dead End Gene Causes Germ Cell Loss and Testicular Germ Cell Tumours." *Nature* 435: 360–364.

Zou, X., Y. He, Z. Zhao, et al. 2025. "Single-Cell RNA-Seq Offer New Insights Into the Cell Fate Decision of the Primordial Germ Cells." *International Journal of Biological Macromolecules* 293: 139136.

Supporting Information

Additional supporting information can be found online in the Supporting Information section. **Figure S1:** Molecular feature of PGC clusters. The results of Gene Ontology (GO) enrichment analysis or KEGG pathway analysis for marker genes of each cluster are shown. The analyzed marker gene source and type of analysis are indicated at the top of each figure (GO(MF); GO enrichment analysis for Molecular Function [MF] category, GO(CC); GO enrichment analysis for Cellular Components [CC] category). (A–C) Results of GO enrichment analysis or KEGG pathway analysis of marker genes of ePGC_E2.5 cluster are shown. (D–F) Results of GO enrichment analysis or KEGG pathway analysis of marker genes of ePGC_E0 cluster are shown. **Figure S2:** Gene expression comparison between cPGC_1w and cPGC_3w. (A) Volcano plots of differentially expressed genes (DEGs) by comparison between cPGC_1w and cPGC_3w are shown. cPGC_1w sample is set as controls. Red plots indicate the upregulated genes (average log2FC > 1, adjusted p-value < 0.01) and blue plots indicate the downregulated genes (average log2FC < -1, adjusted p-value < 0.01). (B) Gene regulatory network (GRN) analysis for DEGs between cPGC_1w and cPGC_3w based on the relation between transcriptional factors (TFs, indicated as triangles) and their known target genes (Target, indicated as circles) is shown. Red arrows in B indicate the genes discussed in the main texts. (C, D) The expression level of MYC (C) and MYCN (D) in each sample is shown. Color value is based on normalized log-transformed value. **Figure S3:** Expression of soma-related genes in PGCs. The expression levels of indicated genes related to heme and tetrapyrrole metabolism (A-D) and neural development (E-H) in each sample are shown. Color value is based on a normalized log-transformed value. **Figure S4:** Molecular characterization of PGC-like cells. The expression levels of indicated germline genes (A-D) and pluripotent marker genes (E, F) in each sample are shown. Color value is based on normalized log-transformed value. **Table S1:** The maker genes of each cluster. **Table S2:** Differentially expressed genes in cPGC_1w_samples. **Table S3:** Number of target genes of TFs in cPGC_1w GRN. **Table S4:** Differentially expressed genes in cPGC_3w_samples compared to ePGC_E2.5. **Table S5:** Number of target genes of TFs in cPGC_3w GRN. **Table S6:** Differentially expressed genes in cPGC_3w samples compared to cPGC_1w. **Table S7:** Tissue-Specific gene expression signatures in DEGs between cPGC_1w versus cPGC_3w.